

Evolutionary model for random plastic analyses of shear-frame buildings using a detailed degradation model

T.L. Attard

Department of Civil Engineering, University of New Hampshire, Durham, NH, USA

M.P. Mignolet

Department of Mechanical and Aerospace Engineering, Arizona State University, Tempe, AZ, USA

Keywords: Bouc and Wen, constitutive models, nonlinear degradation, plastic hinges

ABSTRACT: The random vibration of yielding shear-frame building is considered using a recently proposed detailed degradation model which permits the prediction of the global response of the structure as well as of the state of stress in the members. It is shown that this model can also be used in connection with a global force-displacement model, such as the Bouc and Wen chosen here, to estimate the time evolution of various stress related variables. The two approaches are exemplified on both a single- and a four-story building subjected to ground motions and the corresponding probability density function of response stresses and strains and plastic length are presented and discussed.

1 INTRODUCTION

During strong motion earthquakes, structures can experience large stresses and strains, local failure, and finally collapse. Past earthquakes have proven that plastification does not necessarily develop at the assumed plastic-hinge moment capacities. As such, if the effect of the spread-of-plasticity is not insignificant, inelastic behavior cannot be accurately modeled using zero-length plastic hinge models (Liew et al., 2000). Instead, damage modeled by the gradual spread of yielding through the thickness of the frame member's cross-section and along its length needs considering (Clarke et al., 1991).

To this end, a gradually-degrading and rate-independent hardening model has recently been proposed (Attard, 2005) that is constitutively derived when a material 'just-yields.' Gradual plastification is captured through the section depth and along a member's length. This model is formulated using an integrable stress function defined by a hardening index parameter and a plastic strain coefficient that predict an ultimate failure state through gradual stiffness degradation. A member's inelastic lateral displacements can then be predicted through the post-yield spread (Bayrak and Sheikh, 2001).

The Bouc and Wen model (Bouc 1968, Wen 1976, Baber and Wen 1981) has often been used to predict the smooth degradation of inelastic materials. It has previously been applied in the macroscopic prediction of inelastic phenomena such as pinching (Kunnath et al., 1997) and in the equivalent

linearization approximation of single-degree of freedom systems (Noori et al. 1986, see also Lutes and Sarkani, 1997).

The current investigation focuses on the response of shear-frame building to random ground motion adopting the detailed degradation model of Attard (2005). Accordingly, a perspective on the statistical characteristics of relevant stresses and strains and plastic length can be obtained. In fact, two such approaches can be devised, the first of which relies on the consistent use of the degradation model for the estimation of the displacements and then of the state of stress at any given time. It is however recognized that other models, e.g. the Bouc and Wen model, are available for the prediction of the displacements and may have specific advantages over the present degradation model. For example, the Bouc and Wen is recognized to be well suited for the application of the equivalent linearization approach given its formulation in terms of differential equations. In this light, it is proposed to also investigate the degradation model as a *complement* to an existing displacement prediction model, e.g. the Bouc and Wen model. That is, the time histories of the displacements are first obtained from the Bouc and Wen formulation and then serve as input to the degradation model for the prediction of the detailed state of stress. Both a one- and a four-story shear frame building subjected to Kanai-Tajimi ground motions will serve to exemplify the two approaches discussed above and to provide a perspective on the distribution of some key stress variables.

2 DEGRADATION MODEL

Although gradual degradation models better represent material behavior, e.g., in steel or concrete, than elasto-plastic or bilinear models, the latter are often preferred because of their simplicity. Regardless, the smooth model used here is formulated for a translating yield surface where the back-stress evolution function is given by equation (1) for homogeneous materials where kinematic strain hardening is assumed.

$$\sigma_x = \sigma_{\text{yield}} - \alpha \sigma_{\text{yield}} \left(2 + \frac{1}{\Delta_\epsilon} \right) + \frac{2\alpha \sigma_{\text{yield}} d_x}{e_x} \left(1 + \frac{1}{\Delta_\epsilon} \right) - \frac{\alpha \sigma_{\text{yield}} d_x^2}{\Delta_\epsilon e_x^2} \quad (1)$$

The parameters α and Δ_ϵ may be obtained experimentally and are used to predict the gradual degradation of the material after it yields. For the typical frame member shown in Fig 1, the through-thickness stress distribution through any section is shown; the post-yield stress, σ_x , is found at a depth, d_x . The stress function itself depends on the instantaneous state of post-yield activity, e_x , which is measured as the depth in the cross section that has not yet yielded. The post yield length (PYL) along the member is defined as the ‘spread,’ or portion of the member that has at least ‘just-yielded.’ The PYL is computed using the smooth nonlinear curvature distributions along the member and in accordance with equation (1). The general hysteretic behavior is shown in Fig. 2 for such a member experiencing in-plane, flexural, and uniaxial (σ_x) deformations.

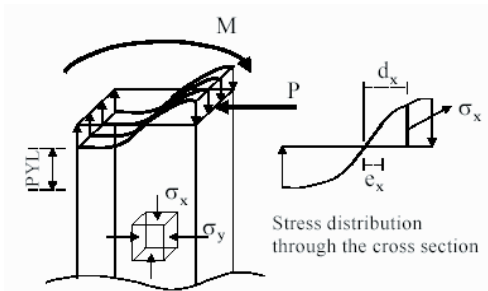


Figure 1. Typical shear frame member

The post-yield deflections relative to each member are then computed where the (maximum) plastic deflection, Δ_p , corresponding to a zero plastic modulus is given by

$$\Delta_p = L \int_0^{\phi_p} f(\Delta\phi) d(\Delta\phi) - \frac{1}{2} \int_0^{\phi_p} f^2(\Delta\phi) d(\Delta\phi) \quad (2)$$

The spread, or PYL, is a function of the post

Top Floor Hysteretic Response of a Four-Story Building Under a Gaussian White Process (Degradation Model)

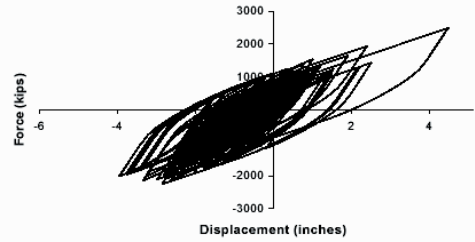


Figure 2. Nonlinear hysteresis for steel ideally assumed as homogeneous

yield curvature, $\Delta\phi$. When the plastic curvature, ϕ_p , is reached in the member (of length L), the spread is identified as the plastic hinge length, L_p . Fatigue-related effects, load-rate effects, P- Δ effects for large axial loads, and anisotropic bi-axial behavior are not treated here, but are currently being investigated.

3 BOUC AND WEN MODEL

The Bouc and Wen model phenomenology is shown in Fig. 3. The smooth hysteretic force $g\{X(t)\}$, which is proportional to the state variable $Z(t)$, responds as the force, $F(t)$, is applied. A linear elastic spring, k_2 , is modeled in parallel with the Bouc and Wen restoring force and is also modeled in series with a friction slider; the elastic-plastic behavior using the slider is intended to prevent a drift in the response, $X(t)$. The system responds according to the steady-state behavior shown in Fig. 2.

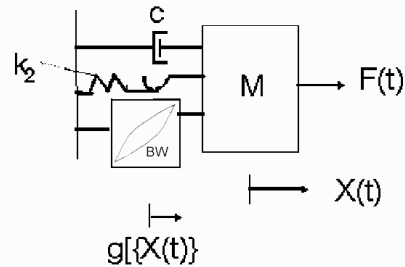


Figure 3. Bouc and Wen system model

The nonlinear equation of motion is shown in equation (3), where m and c denote the system’s mass and damping, respectively.

$$m \ddot{X} + c \dot{X} + k_2 X + g\{X(t)\} = F(t) \quad (3)$$

The constitutive model of equation (1) leads to various levels of plastic straining in the member depending on when unloading occurs in the member.

Because of the random nature of the excitation, this level can be discretely defined at high-, medium-, and low-levels of straining. Specifically applying the parameters $\alpha=0.2$ and $\Delta\epsilon = 14$ (see Attard, 2005) to a steel (Grade A36; $\sigma_y=36$ ksi; ideally homogeneous) shear frame member (Fig. 1), hysteresis loops for quasi-static amplitudes can be generated. Each member is 120 inches long, and has cross-sectional dimensions of 10 inches (strong axis) by 22 inches. The parameter α defines the average plastic modulus between the ‘just-yielded’ and the ‘ultimate’ states of plastification; the plastic strain coefficient measures the ultimate strain after ‘just yield.’ The plastic hinge length, L_p , is determined as 47.741 inches. The four Bouc and Wen model parameters are then optimally determined using a Gauss-Newton algorithm. The degradation model’s restoring force is defined by $g[\{X(t)\}]$, the Bouc and Wen force is Z , and the Bouc and Wen parameters n , A , α , and β are determined so the error in the two models is minimized. The optimal Bouc and Wen parameters are $n=0.55$, $A=1167.138$, $\alpha=14.308$, and $\beta=0.759$ for all levels of post-yield behavior - low-level ($5\epsilon_y$), mid-level ($8\epsilon_y$), and high-level ($14\epsilon_y$) of strain, where the ultimate strain is $\epsilon_u=15\epsilon_y$ ($\Delta\epsilon = 14$) at the outermost fiber at the member tip. A typical comparison of the hysteresis loops corresponding to the degradation model and its best fit Bouc and Wen approximation is shown in Fig. 4.

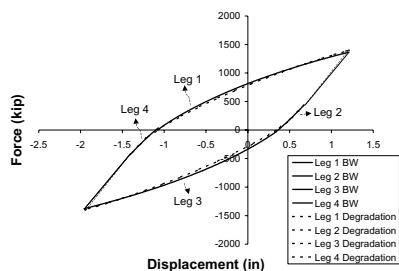


Figure 4. Comparison of hysteresis curves obtained from the degradation model and its best fit Bouc and Wen approximation. High level straining.

4 NUMERICAL EXAMPLES

The detailed degradation and Bouc and Wen models discussed above were first applied to a single-degree-of-freedom model consisting of a mass of $0.5k\text{-s}^2/\text{in}$ supported by a 120 in column with a stiffness of $1787k/\text{in}$. The elastic natural frequency of this system was found to be 9.51Hz, and a 5% damping ratio was assumed to be present. The

degradation model was characterized by $\alpha=0.2$ and $\Delta\epsilon=14$ where the ultimate strain ($15\epsilon_y$) was specified at 15 times the yield strain. Further, this system was subjected to different random excitations modeled as Gaussian stochastic processes with Kanai-Tajimi spectra (see Clough and Penzien, 1993) of parameters given in Table 1. The response of the single-degree-of-freedom system was marched in time from zero initial condition by the Newmark Beta scheme with linear acceleration with a time step of 0.02 s until a final time of 40s. 360 such records were produced and the transient component of the response was discarded in all cases. The results shown in Fig. 5 and 6 are obtained by averaging over the entire set of records.

Table 1. Parameters of the Kanai-Tajimi spectra used as excitation.

Excitation	ω_g (rad/sec)	ξ_g	G_0
KT1	15.60	0.60	0.098
KT2	27.00	0.34	0.07
KT3	46.22	0.34	0.07

Shown in Fig. 5 are the power spectra of the tip displacement corresponding to all three excitations obtained by an autoregressive modeling of the data with model order of 100 (see Marple, 1987). Note that the peak of the Kanai-Tajimi spectra of excitation KT1 and KT2 is away from the single-degree-of-freedom resonance, and thus two separate peaks are observed with the lowest corresponding to the peak of the excitation spectrum and the highest associated with the natural frequency of the system. The excitation KT3 had a peak frequency close enough to the natural frequency of the single-degree-of-freedom to induce a single, broad peak in the displacement spectrum, see Fig. 5. No noticeable harmonic of the natural frequency was observed. Finally, the sharp peak at the zero frequency seen on Fig. 5 is believed to be associated with the relatively short length of each of the 360 records produced and the lack of mean removal in the autoregressive modeling effort.

The probability density function of the response was estimated next, see Fig. 6(a). For the excitations KT1 and KT2, it was found that the distribution of the displacement is almost Gaussian with kurtosis of 2.99 and 3.15, respectively. For the resonant, KT3 excitation, a significantly non-Gaussian distribution is obtained, see Fig. 6(a), with kurtosis of 3.63. The increasing deviation of the kurtosis from the Gaussian value of 3 suggests an increasing level of nonlinearity/plastic deformation which is consistent with the increased level of response to KT3 vs. KT2 vs. KT1, see Fig. 5. Notwithstanding the close Gaussianity of the probability density function of the

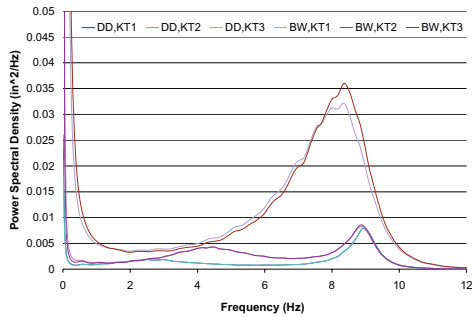


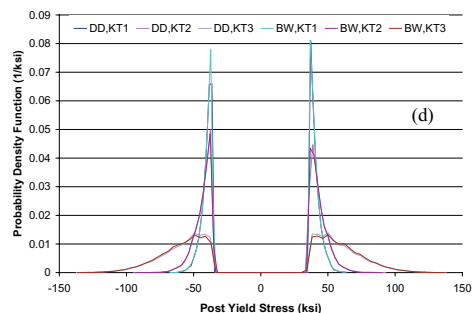
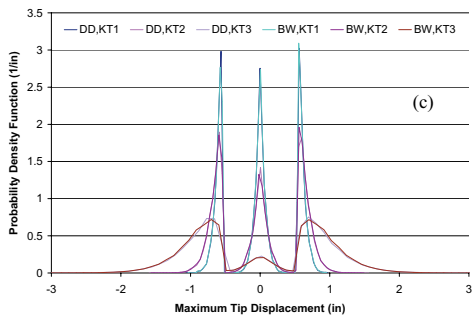
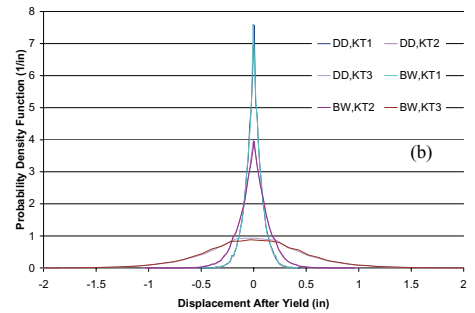
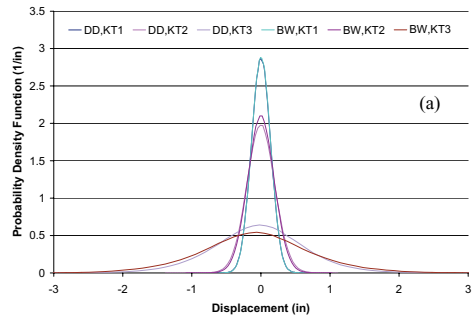
Figure 5. Power spectral density of the single-degree-of-freedom displacement for both the detailed degradation (DD) and Bouc and Wen (BW) models and for all three Kanai-Tajimi excitations (see Table 1).

response corresponding to the excitations KT1 and KT2, there exists a significant number of plastic excursions in the time histories.

A first perspective on the plastic deformations induced can be obtained from the maximum displacement after yield the probability density function of which is shown in Fig. 6(b). This symmetric distribution exhibits a peak near zero which is consistent with the distributions of Fig. 6(a), i.e. that small excursions are most likely than large ones. As the level of response increases (KT3 vs. KT2 vs. KT1), the spread of the distribution increases as large deformations become more likely. A more rich description of the motion can be obtained by considering the “maximum tip displacement” which is here defined as the difference between the total displacements of two consecutive plastic excursions. Its distribution, see Fig. 6(c), reveals two distinct regions: the values between -0.54 in and 0.54 in and those outside of this band. In fact, 0.54 in corresponds to twice the tip displacement required to yield the column so that a maximum tip displacement less in magnitude than this threshold can only be accomplished if the two consecutive plastic excursions occur on the same side of the neutral axis of the column. Conversely, maximum tip displacement values exceeding 0.54 in in magnitude are often, but not always, indicative of a motion from one side of the column to the other. As the response level is increased, i.e. from KT1 to KT2 to KT3, the probability of a same side reloading/ reyielding decreases, see Fig. 6(c). This result is expected as these large excursions become more probable. In addition, it may be argued that the response to the KT3 excitation is fairly narrowband and thus exhibits a strong component of frequency close to 9Hz to which is associated motions from one side to the other, thereby favoring opposite side reyielding.

A particularly interesting feature of the

degradation model is its capability to provide a perspective on the state of stress in the column. It



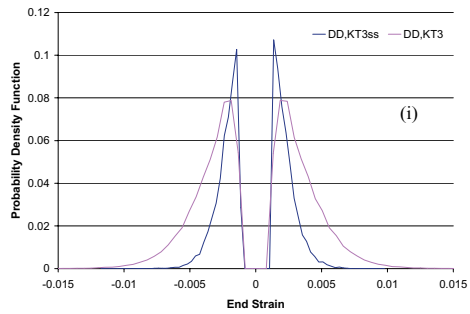
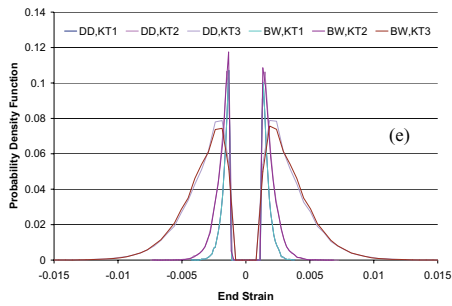
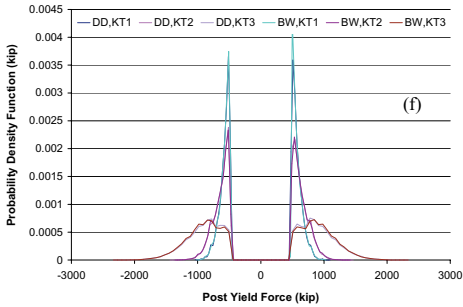
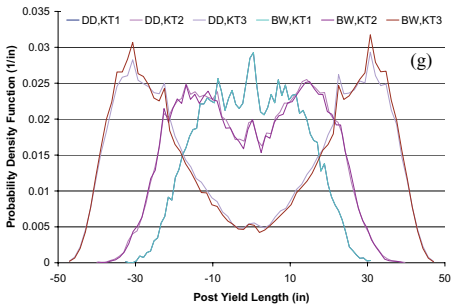


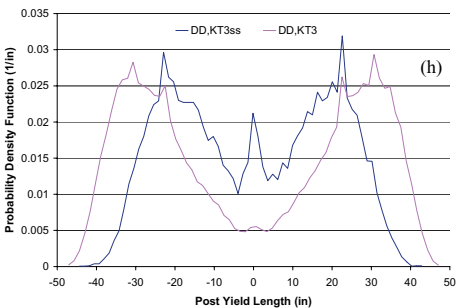
Figure 6. Probability density functions of response. (a) displacement, (b) maximum displacement after yield, (c) maximum tip displacement, (d) post yield stress, (e) end strain, (f) post yield force, (g) post yield length, (h) and (i) post yield length and end strain for same side reloading.



(f)



(g)



(h)

permits in particular the monitoring of such quantities as the stress and strain at the tip fiber at the ends of the column and the shear force at those same locations (referred to here as the post yield stress, the end strain, and the post yield force, respectively) as well as the length of the plastic zone (denoted here as the post yield length). The probability density functions of these variables are shown in Fig. 6(d)-(g) for the three excitations considered. The post yield stress, end strain, and post yield force distributions exhibit similar features, i.e. they are zero in a middle region which corresponds to elastic motions and have a sharp peak at or very close to the yielding threshold. The probability density functions then decrease reflecting the same trend of the displacement distribution, see Fig. 6(a).

The probability density function of the post yield length is however quite different as it is characterized by two side peaks that increase in magnitude and shift toward larger values (in magnitude) as the response level is increased.

Having noted, see Fig. 6(c), the specificity of the same side reyielding, it was questioned whether and how these events might affect the distribution of the post yield variables. To this end, the occurrences of same side reyielding were singled out and the probability density functions of the end strain and post yield length conditional on this event were estimated, see Fig. 6(h) and (i). Surprisingly, it was found that these conditional distributions (labeled DD,KT3ss, with ss for same side) are in fact similar in shape to their unconditional counterparts (labeled DD,KT3) but exhibit a smaller spread from the yielding threshold. This property is in fact expected from the plasticity model adopted here as a reloading to the same position/displacement as in the previous plastic cycle corresponds in fact to simply

attaining the yield point (and thus a post yield length of zero) irrespectively of the level of plastic deformations that were achieved in this previous cycle at the same displacement. Thus, achieving twice consecutively the same post yield length on the same side requires on the second event a much larger displacement than on the first. On the contrary, obtaining the same post yield length (in magnitude) on the opposite side of the column neutral axis only requires an equal displacement but of opposite sign. This difference in behavior suggests that the all plastic state variables, e.g. post yield length and end strain, will exhibit smaller values for the same side reyielding as compared to opposite side reyielding, see Fig. 6(h) and (i).

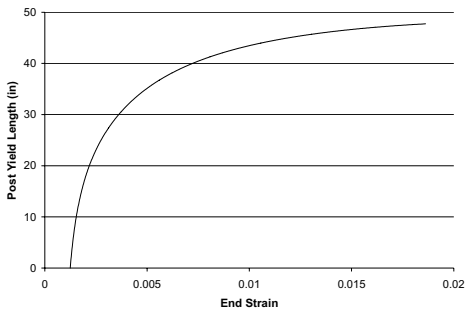


Figure 7. Post yield length as a function of the end strain.

The clarification of the features of the distribution of the post yield length lies in fact in the memoryless transformation between the end strain and the post yield length, see Fig. 7. Specifically, a small interval of end strains near the yielding threshold is mapped into a much larger post yield length domain resulting in a decrease of the probability density function. Conversely, a large increase in end strain only leads to a small increase in post yield length, thereby boosting the value of the probability density function. So, the large values of the probability density function of the end strain near the yielding threshold are scaled down by the transformation while the low values at large strains are scaled up. This process results in a dramatic shift of the peak of the distribution, from the neighborhood of the yielding point for the end strain to a value near the formation of a plastic hinge for the post yield length.

An important aspect of the present effort was on the comparison of the Bouc and Wen model with separate elastic component (see Fig. 3) and the detailed degradation model. Three questions were of particular interest:

(a) are the displacement properties (probability density function, power spectral density) similar for the degradation model and an appropriately fitted (see

above) Bouc and Wen representation?

(b) is it possible to use the detailed degradation model to *complement* the Bouc and Wen representation, i.e. to post-process the time histories obtained by this model to obtain end strains, post yield length, etc.?

(c) if so, how good is this post-processing as compared to the use of the detailed degradation model for both displacement and stress prediction?

Figures 5 and 6(a) provide a first, positive answer to the first question. A comparison of the curves labeled DD (detailed degradation) and BW (Bouc and Wen) of these figures suggests that the two models provide a similar characterization of the response with the coefficients of the fitted Bouc and Wen model given earlier.

Since the detailed degradation model estimates the state of stress from the displacement time history, the answer to question (b) is most certainly yes and the accuracy (see (c)) can be assessed from Fig. 6(b)-(f). In fact, it is seen that the Bouc and Wen model provides a good to very good fit of these results with an accuracy that appears to be slightly decreasing as the level of response is increased.

In this light, it is possible to use either the degradation model alone or in concert with a more global description of the plastic behavior of the member (the Bouc and Wen model here) to obtain time histories of displacements and stresses.

A further validation of the above findings was obtained by considering a 4-story shear building with masses and columns all identical to their single-degree-of-freedom counterparts. The natural frequencies of this structure were found to be 3.30, 9.51, 14.58, and 17.88 Hz. The random response of this building to the excitation KT1 was obtained under the assumption of classical damping with 5% damping ratios. The computational details are similar to those of the single-degree-of-freedom example except for the number of records considered which was selected to be 300.

Given that the dominant frequency of the excitation was close to the lowest natural frequency of the structure, a large, resonant response was observed which resulted in large and/or numerous plastic excursions. Since the motivation for this 4-degree-of-freedom case was the validation of the above findings, not a discussion of the failure (e.g. its probability and/or the statistics of the time to failure), it was assumed that the force-displacement curve extended past the formation of a plastic hinge with a constant slope. However, the plasticity indicators (post yield length, stress, force, and end strains) were limited to their value corresponding to the formation of a plastic hinge.

The displacement spectra obtained from the degradation model were first examined, see Fig. 8. It is found that the response of the system is dominated

by the first mode but that the peak of the spectrum has shifted from the corresponding linear natural frequency (3.3Hz) to approximately 2.3 Hz because of the softening induced by the inelastic deformations.

Next, the probability density functions of the variables considered earlier (i.e. maximum tip displacements, displacements after yield, post yield stresses, end strains, post yield forces, and post yield lengths) of the degrees-of-freedom 1 (top) and 2 or of the columns between degrees-of-freedom 1 and 2, and 2 and 3 were analyzed and found to be completely consistent with their counterparts from the single-degree-of-freedom analysis, see Fig. 6(a)-(g). Higher stresses were however observed on the two remaining columns, between degrees-of-freedom 3 and 4 (bottom) and 4 and ground and the corresponding probability density functions of the maximum tip displacements, post yield stresses, end strains, post yield forces, and post yield lengths are shown in Fig. 9(a)-(e). These plots provide an extension of the distributions of Fig. 6(c)-(g) to higher levels of response and follow the trends already noted in connection with the single-degree-of-freedom system.

The applicability of the fitted Bouc and Wen model was again demonstrated as the displacements and stresses predicted from it and those corresponding to the detailed degradation model match well to very well, as in the single-degree-of-freedom case, see Fig. 9(a)-(e).

Finally, an investigation of the time to the formation of the first plastic hinge was initiated to complement the above stationary analysis. Shown in Fig. 10 is the probability density function of this time for the single-degree-of-freedom system excited by the Kanai-Tajimi ground motions KT3 with $G_0=0.126$. Note the strong exponential character of this distribution starting from a lower threshold time. The distribution of the displacement after yield obtained at hinging, not shown here for brevity, shows trends similar to the probability density functions of Fig. 6(b)-(f), i.e. a rapid

(exponential-like) decrease for values larger in magnitude than the threshold corresponding to hinging (2.75 here) and zero for values in the domain $[-2.75, 2.75]$.

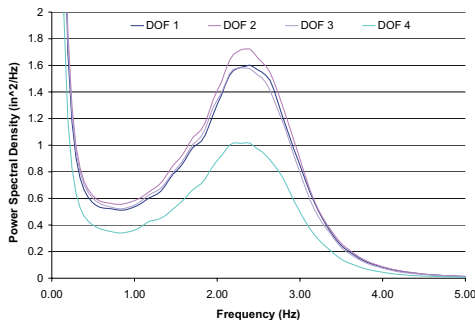
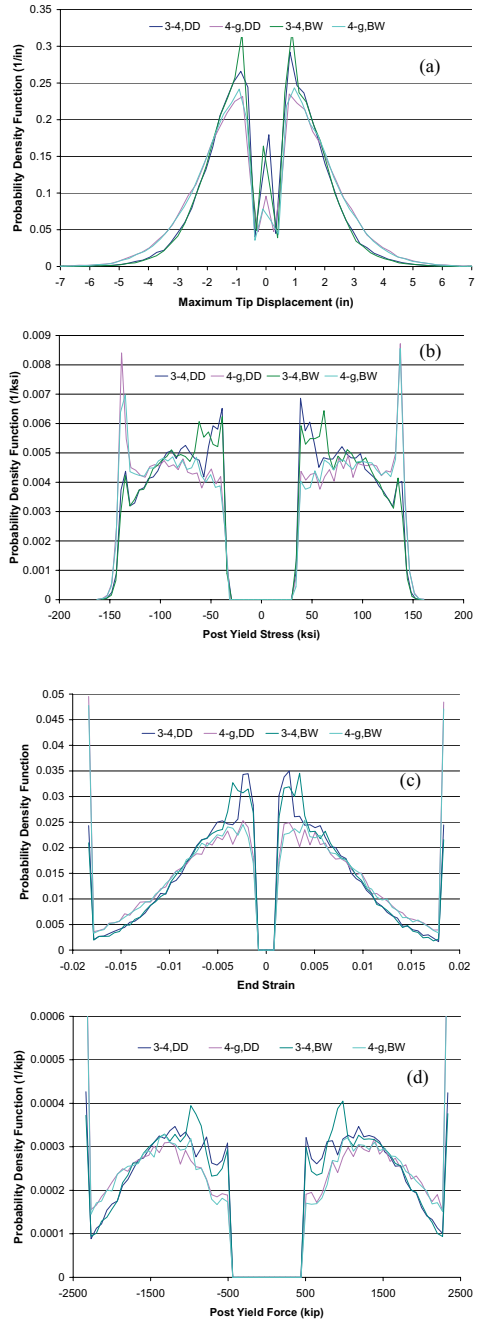


Figure 8. Power spectral density of the displacements of all degrees-of-freedom for the detailed degradation model.



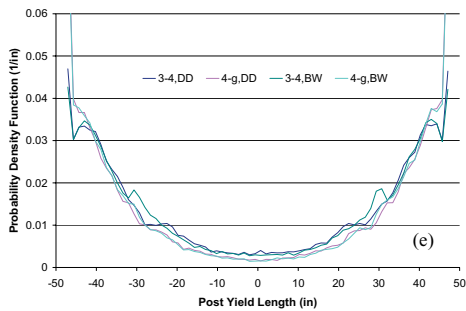


Figure 9. Probability density functions of (a) maximum tip displacement, (b) post yield stress, (c) end strain, (d) post yield force, and (e) post yield length, in the columns between degrees-of-freedom 3 and 4 (3-4) and degree-of-freedom 4 and the ground (4-g) obtained with the detailed degradation (DD) and Bouc-Wen (BW) models.

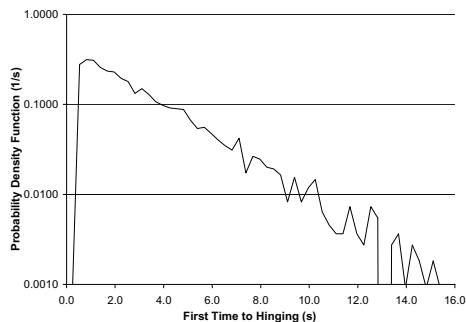


Figure 10. Probability density function of the first time to hinging.

5 CONCLUSIONS

The primary focus of this investigation was on the validation of a recently developed detailed degradation model for the prediction of the response of yielding shear frame building subjected to random excitations. This detailed degradation model permits the prediction of the global features of the response, e.g. displacement time histories, but also provides a perspective on the state of stress in the structural members, e.g. end strain, post yield stress, post yield length. The use of this model was demonstrated on both a single-degree-of-freedom system and a 4-story building and the corresponding probability density functions of the various displacement and stress based variables were presented and discussed.

It was further noted that this detailed degradation model can be successfully used either in place of or in conjunction with a global force-displacement representation such as the Bouc and Wen model. In the latter case, the displacement time history is first

obtained from the global model and this data is then post processed by the degradation model to provide an estimate of the corresponding stress state in the members. The accuracy of this two step approach was confirmed on the single- and 4-degree-of-freedom systems by first obtaining a Bouc and Wen model closely fitting the force-displacement relation of the degradation model past yield. The very satisfactory matching of the probability density functions and power spectra of all response quantities, displacement and stresses, obtained by this approach and directly from the degradation model then demonstrates the applicability of the detailed degradation model in conjunction with a more global model.

ACKNOWLEDGEMENT

The computational assistance of Messrs. Anthony Agelastos and Bo Yang is gratefully acknowledged.

REFERENCES

- Attard, T., 2005. Post-Yield Material Nonlinearity: Optimal Homogeneous Shear- Frame Sections and Hysteretic Behavior, Accepted, *International Journal of Solids and Structures*.
- Baber, T., & Wen, Y. 1981. Random vibration of hysteretic degrading systems, *Journal of Engineering Mechanics, ASCE*, Vol. 107 (No. 6): 1069-1087.
- Bayrak, O., & Sheikh, S. 2001. Plastic hinge analysis, *Journal of Structural Engineering*, Vol. 1279: 1092-1100.
- Bouc, R. 1968. Forced vibration of a mechanical system with hysteresis, Abstract in *Proc. of the Fourth Conference on Nonlinear Oscillations*, Academia Publishing, Prague, Czechoslovakia: 315.
- Clarke, M., Bridge, R., Hancock, G., & Trahair, N. 1991, Design using advanced analysis, *SSRC Annual Tech. Session Proc.*, Lehigh, Univ., Bethlehem, PA.: 27-40.
- Clough, R.W., & Penzien, J. 1993. *Dynamics of Structures*, Second Edition, McGraw-Hill, New York.
- Kunnath, S., Mander, J., & Fang, L. 1997. Parameter identification for degrading and pinched hysteretic structural concrete systems, *Engineering Structures*, Vol. 19 (No. 3): 224-232.
- Liew, J., Chen, H., Shanmugam, N., & Chen, W. 2000. Improved nonlinear plastic hinge analysis of space frame structures, *Engineering Structures*, Vol. 22 (No.10): 1324-1338.
- Lutes, L. & Sarkani, S. 1997. *Stochastic Analysis of Structural and Mechanical Systems*, Prentice Hall, Upper Saddle River, NJ.
- Marple, S.L., 1987. *Digital Spectral Analysis with Applications*, Prentice-Hall, Englewood Cliffs.
- Noori, M, Choi, J., & Davoodi, H. 1986. Zero and non-zero mean random vibration analysis of a new general hysteretic model, *Probabilistic Engineering Mechanics*, Vol. 14: 192-201.
- Wen, Y. 1976. Method for random vibration of hysteretic systems, *Journal of the Engineering Mechanics Division*, Vol. 102 EM2: 249-262.